Vision-only Navigation and Control of Unmanned Aerial Vehicles Using the Sigma-Point Kalman Filter

Houwu Bai, Eric Wan, Xubo Song, Andriy Myronenko
Department of Computer Science & Electrical Engineering, OGI School of Science & Engineering, OHSU
Alexander Bogdanov
Department of Interactive and Autonomous Systems at Teledyne Scientific Company

BIOGRAPHY

Houwu Bai is a Ph.D. student in the Department of Computer Science & Electrical Engineering, OGI School of Science & Engineering, OHSU. His research interests include intelligent signal processing and applications. He received his B.S. degree in Xi'an Jiaotong University, Xi'an China in 1995 and M.S. degree in the Institute of Automation of the Chinese Academy of Sciences, Beijing China in 1998.

Eric Wan is an Associate Professor in the Department of Computer Science and & Electrical Engineering, OGI School of Science and Engineering, OHSU. He received his BS (1987), MS (1988), and Ph.D. (1994) in Electrical Engineering from Stanford University. His research is in algorithms and architectures for adaptive signal processing and machine learning. He has ongoing projects in autonomous unmanned aerial vehicles, estimation and probabilistic inference, integrated navigation systems, time series prediction and modeling, and speech enhancement. He holds several patents in adaptive signal processing and has authored over 60 technical papers in the field.

Xubo Song is an assistant professor in the Department of Computer Science and Electrical Engineering, at the OGI School of Science and Engineering, Oregon Health and Science University. She obtained Master and Ph.D. degrees in 1994 and 1999 respectively, both in Electrical Engineering from California Institute of Technology. Her research interests include machine learning, and image processing and analysis.

Andriy Myronenko is a Ph.D. student in the Department of Computer Science & Electrical Engineering, OGI School of Science & Engineering, Oregon Health and Science University. He received his B.S. and M.S. degrees in Dnepropetrovsk National University, Dnepropetrovsk Ukraine in 2004 and 2005 respectively.

Alexander Bogdanov is a Research Scientist in the Department of Interactive and Autonomous Systems at Teledyne Scientific Company. His research interests include autonomous vehicle control, estimation, and navigation. He obtained his MS degree in electrical engineering in 1994, and his Ph.D. in engineering in 1998, both from Baltic State Technical University, St. Petersburg, Russia.

ABSTRACT

This paper presents the vision-only navigation and control of a small autonomous helicopter given only measurements from a video camera fixed on the ground. The goal is to develop an alternative to traditional INS/GPS and on-board vision aided systems.

The autonomous navigation and control of the helicopter is achieved using a nonlinear state estimator and a state-dependent controller. A key difference to INS/GPS navigation is that measurements of the helicopter's accelerations and angular velocities are not directly available. The state estimation combines the vision measurements with a dynamic model of the vehicle in a recursive filtering procedure using a Sigma-Point Kalman Filter (SPKF). The estimation of the helicopter's current state (position, attitude, velocity, and angular velocity) is then fed back in real-time to a state-dependent Riccati equation (SDRE) controller to generate radio control commands to the helicopter.

Simulations are provided comparing performance relative to INS/GPS navigation. Experiments also show that an accurate dynamic model of the vehicle is necessary for closed-loop stability. Our results indicate the feasibility of designing a vision-only estimation and control system capable of stabilizing and maneuvering a small unmanned helicopter.

Other than simple on-board avionics for low level actuator control, the ground station is responsible for video capture, state-estimation, and state-feedback flight control.

1. INTRODUCTION

Vision has been used in conjunction with inertial sensors, GPS receivers, or other sensors in the development of unmanned aerial vehicles (UAVs) for the purpose of accurate 3D positioning, attitude estimation, UAV autonomous landing, path planning, and UAV situation awareness and collision avoidance [Ref. 5, 6, 11, 17, 19, 22, 25, 28]. However, the **vision-only** navigation and control of UAVs has been investigated by only a few researchers. The vision-only approach and landing of a GTMax helicopter was presented in Ref. 20. The vision-only control and navigation of a small glider was presented in Ref. 21. While promising results were reported for the given applications, there are several limitations in these works. A simplified process model that assumed constant velocity and constant angular acceleration was applied in Ref. 21. For the small glider, only limited maneuvers are possible. Both approaches only considered on-board vision systems.

In this paper, we present the vision-only navigation and control of a small autonomous helicopter given only measurements from a video camera fixed on the ground. A typical application would involve landing a UAV using simply a camera fixed on the landing pad. Since the on-board avionics can be greatly simplified (*i.e.*, no inertial measurement unit), the approach may present significant cost benefits for controlling small UAVs.

Our approach combines a state estimator using a Sigma-Point Kalman Filter (SPKF) with only vision measurements and a SDRE controller. In contrast to previous approaches, the helicopter's complete state, which includes the position, attitude, velocity, and angular velocity, is estimated given only vision measurements from a camera fixed on the ground. Furthermore, the state estimate is fed back in real-time to a state-dependent Riccati equation (SDRE) controller to stabilize the helicopter and to generate the desired control commands.

In the following sections, we will first present the state estimation component, which includes aspect of dynamic modeling, vision, and the SPKF. We then provide a short review of the SDRE controller, followed by experimental results, and finally conclusion and future work.

2. STATE ESTIMATION

The state estimation is formulated based on the following dynamic state space model.

$$x_{k+1} = f\left(x_k, u_k, n_k^f\right) \qquad (1)$$

$$y_k = h\left(x_k, n_k^h\right) \qquad (2)$$

where x is the vehicle state, y is the observation, u is the controller signal, f is the process model, h is the measurement model, and n^f and n^h are process noise and measurement noise, respectively.

For the UAV, the state vector is defined as

$$x = \left[v^T \ w^T \ p^T \ q^T\right]^T \qquad (3)$$

where v is the vehicle's velocity, w is the angular velocity in the body frame, p is the position in the navigation north-east-down (NED) frame, and q is the attitude quaternion.

Estimation of the vehicle's state requires formulating the process model f of vehicle motion, the measurement model h of the video observations y, and an inference algorithm to calculate the state estimation given the models and observations.

As the basis of the process model for UAV navigation, the following kinematic equations describe the vehicle's motion irrespective of the forces that produce the motion [Ref. 27]:

$$\dot{v} = C_n^b g + a^v \qquad (4)$$

$$\dot{w} = a^w \qquad (5)$$

$$\dot{p} = C_b^n v \qquad (6)$$

$$\dot{q} = \frac{1}{2} q \bullet r \qquad (7)$$

where g is the acceleration due to the gravity, a^v is acceleration other than the gravity applied on the vehicle, a^w is the angular acceleration. C_n^b and C_b^n are the navigation-to-body frame and the body-to-navigation frame direction cosine matrix (DCM), respectively. The auxiliary quaternion vector r is defined as $r = \left[0, w^T\right]^T$; the quaternion product is denoted by '$\bullet$'. The DCM, quaternion, and Euler angle are three equivalent representations of the vehicle's attitude [Ref. 27 section 3.6].

The discrete-time updates for position, velocity, and angular velocity are calculated by the following first-order Euler update:

$$p_{k+1} = p_k + dt\,\dot{p}_k + n_k^p \qquad (8)$$

$$v_{k+1} = v_k + dt\,\dot{v}_k + n_k^v \qquad (9)$$

$$w_{k+1} = w_k + dt\,\dot{w}_k + n_k^w \qquad (10)$$

where dt is the time-step of the discrete-time system, n^p, n^v, and n^w are process noise for position, velocity, and angular velocity, respectively. The discrete-time update for the quaternion is calculated using the attitude computation algorithm presented in section 10.2 of Ref. 27.

2.1 PROCESS MODELS

For INS/GPS integrated navigation, the full process model is formulated by combing the kinematic equations with the sensor model of the inertial measurement units (IMUs). However, in the vision-only approach, the IMU is absent, and direct measurements of the helicopter's accelerations and angular velocities are not available. In this paper we consider both a **stochastic model** and a **dynamic model**.

2.1.1 Stochastic model

In the tracking literature there are several ways to approximate the target motion by stochastic processes [Ref. 12]. For example, we can approximate the acceleration and angular acceleration by the following random process.

$$a_{k+1} = \alpha\,a_k + n_k^a \qquad (11)$$

where n^a is white Gaussian noise, and $\alpha \le 1$ is a low-pass parameter. The stochastic approximation is applied for the acceleration a^v and angular acceleration a^w of the kinematic model. Equation (11), combined with equation (4)-(7), specifies a complete process model necessary for the state estimation framework.

2.1.2 Dynamic model

Since we also have available a full dynamic model of the vehicle (used for simulation and control), we may also employ this full model for state estimation. As it will be shown, applying the helicopter's dynamic model is crucial for the vision-only navigation and control.

The helicopter's dynamic model is described as a generic 6DOF rigid body model with external forces and moments originating from the main and tail rotors, empennage and fuselage drag [Ref. 7].

$$\dot{v} = C_n^b g + \frac{F}{m} + v \times w \qquad (12)$$

$$\dot{w} = -I^{-1} w \times I w + I^{-1} M \qquad (13)$$

where m is the helicopter's mass, I is the angular inertial matrix and assumed to be diagonal. The vector cross product is denoted by '$\times$', forces and moments acting on the helicopter are denoted by F and M, respectively.

To complete the description of the model, the forces and moments acting on the helicopter must be specified.

$$F = \begin{pmatrix} X_{mr} + X_{fus} \\ Y_{mr} + Y_{fus} + Y_{tr} + Y_{vt} \\ Z_{mr} + Z_{fus} + Z_{ht} \end{pmatrix} \qquad (14)$$

$$M = \begin{pmatrix} L_{mr} + L_{vt} + L_{tr} \\ M_{mr} + M_{ht} - Q_{tr} \\ -Q_e + N_{vt} + N_{tr} \end{pmatrix} \qquad (15)$$

where $(X, Y, Z, L, M, N)_{mr, tr, fus, vt, ht}$ are forces/moments due to the main rotor, the tail rotor, the fuselage, the vertical fin and the horizontal stabilizer of the helicopter. The engine torque and the tail rotor torque are represented by Q_e and Q_{tr}. These components can be calculated given two inputs 1) the velocity and angular velocity of the vehicle, and 2) the control commands low-pass filtered by the helicopter's servo model.

To calculate the moments of the main rotor, the main rotor's lateral and longitudinal flapping dynamics can not be neglected. The lateral and longitudinal flapping dynamics are presented by the first-order equations:

$$\dot{b}_1 = -p - \frac{b_1}{\tau_e} - \frac{\partial b_1}{\partial \mu_v} \frac{v - v^w}{\tau_e V_{tip}} + K_{lat} u_{lat} \qquad (16)$$

$$\dot{a}_1 = -q - \frac{a_1}{\tau_e} + \frac{\partial a_1}{\partial \mu} \frac{u - u^w}{\tau_e V_{tip}} + \frac{\partial a_1}{\partial \mu_z} \frac{w - w^w}{\tau_e V_{tip}} + K_{lon} u_{lon} \qquad (17)$$

where $v = (u\ v\ w)^T$, $v^w = (u^w\ v^w\ w^w)^T$, and $w = (p\ q\ r)^T$ are components of velocity, wind velocity, and angular velocity. The lateral and longitudinal control inputs are represented as u_{lat} and u_{lon}. The damping time constant for the flapping motion is $\tau_e \approx 0.1$sec. The tip speed of the main rotor is $V_{tip} \approx 125$m/sec.

The engine torque Q_e in equation (15) is calculated using the following equations

$$Q_e = \frac{P_e^{\max}}{\Omega} \delta_t \qquad (18)$$

$$\delta_t = K_p\left(\Omega_c - \Omega\right) + K_i I_\Omega \qquad (19)$$

$$\dot{I}_\Omega = \Omega_c - \Omega \qquad (20)$$

where $P_e^{\max}$ is the maximum engine power, δ_t ($0 < \delta_t < 1$) is the throttle setting, Ω_c is the rotor speed command, Ω is the rotor speed, which is assumed measurable. I_Ω is the integrator of the difference between the rotor speed command and the actual rotor speed. The integrator is reset whenever the computed throttle command is saturated.

For additional details on how to calculate the moments (L, M, N) and forces (X, Y, Z), the reader is referred to Ref. 7. Note that most of the model parameters in the dynamic model have a clear physical meaning and are relatively easy to adapt to different rotorcraft vehicles.

In summary, Equations (6)-(7) and (12)-(13) with associated equations to calculate the forces and moments completely specify the dynamic model used for inference. Note that the state vector $x = \begin{bmatrix} v^T & w^T & p^T & q^T \end{bmatrix}^T$ is augmented with the internal state variables $\begin{bmatrix} b_1, & a_1, & I_\Omega \end{bmatrix}^T$, which must also be estimated by the inference algorithm.

2.2 THE VISION MEASUREMENTS AND THE OBSERVATION FUNCTION

A fixed video camera mounted on the ground is used to capture the helicopter in flight. For this initial work, we extract the vision measurements from simulated video. An example video frame is shown in Fig. 1.

Fig. 1. An example simulated image

In Fig. 1, our vision measurements are the feature points, shown as red dots. The 2D locations of the feature points, which represent observations y in equation (3), are extracted from the rendered images based on color and shape differences. These 2D feature points in the image are generated in OpenGL by projecting a set of pre-defined 3D feature points to 2D based on the camera's parameters and the helicopter's position and attitude.

To estimate the helicopter's state, the observation function h in equation (3), which calculates the predicted measurements given previous state estimates also has to be formulated. The observation function results from the projection of the 3D feature points to the 2D image plane [Ref. 16], and is composed of the following three steps:

1) Transform the 3D location of the feature point from the body frame to the navigation frame.

$$l_n = C_b^n l_b + p \qquad (21)$$

where l_n and l_b are the 3D location of a feature point in the navigation frame and the body frame, respectively. This transformation is explicitly dependent on the position p and attitude C_b^n of the vehicle.

2) Transform from the navigation frame to the camera frame.

$$l_c = R\left(l_n - l_{cam}\right) \qquad (22)$$

where l_{cam} is the location of the fixed camera in the navigation frame, R is the coordinates transformation matrix from the navigation frame to the camera frame.

3) Project to image plane using a projective projection.

$$l_{2D} = \frac{r_y}{2\tan\left(\theta/2\right)} \frac{1}{l_c(3)} \begin{pmatrix} l_c(1) \\ l_c(2) \end{pmatrix} \qquad (23)$$

where θ is the vertical view angle of the camera, r_y is the vertical resolution of the image. Here a pinhole camera model is used.
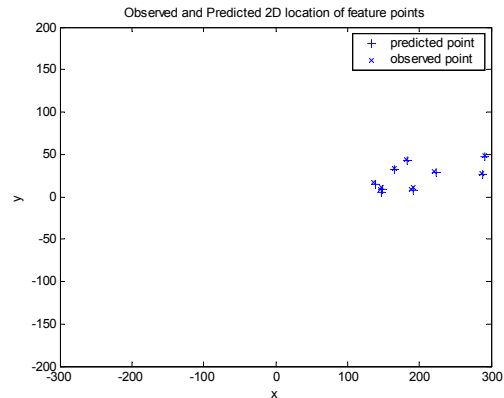

Fig. 2. Observed and predicted 2D locations of feature points

In the Kalman framework for state estimation, the innovations, which is used for the measurement updates, is given by the difference between the observed location of the feature points and the predicted location of the feature points. To evaluate this, however, the point-to-point correspondence between the two sets of points must be established. Correspondence between the observed points and the predicted points is resolved using the Scott and Longuet-Higgins algorithm [Ref. 23]. The algorithm has a straightforward implementation founded on a well-conditioned eigenvector solution, which involves no explicit iterations. The algorithm can be briefly summarized in following steps: 1) Build a proximity matrix for all possible feature pairs, where each element is Gaussian-weighted distance between two points. 2) Compute the singular value decomposition of the proximity matrix, replace all singular values by one, and compose a new proximity matrix. The achieved matrix has the property of amplifying good pairings. 3) The element greatest in its row and column shows that corresponding two features are in correspondence with one another. The algorithm works well with translation, scaling deformations, and with moderate rotations, and thus was sufficient for our rigid-body correspondence estimation.

2.3 THE SIGMA POINT KALMAN FILTER (SPKF)

The Kalman filter provides a recursive procedure to optimally combine noisy observations with predictions from the process model. Though the Kalman filter generates optimal estimates in linear dynamical systems, its nonlinear counterpart, the Extended Kalman Filter (EKF), only provides approximate maximum likelihood estimate of the state of a nonlinear system [Ref. 8]. In the EKF, the system state and noise densities are approximated by Gaussian Random Variables (GRV), which are propagated through a first order linearization of the nonlinear system. This can lead to large errors in the true posterior mean and covariance of the transformed GRV, which may lead to suboptimal performance and sometimes causes divergence of the filter.

Sigma-Point Kalman Filters (SPKF), which include the Unscented Kalman Filter (UKF) [Ref. 10], Central Difference Kalman Filter (CDKF) [Ref. 18], and their square-root variants [Ref. 14], have recently become a popular better alternative to the EKF [Ref. 13, 14, 15]. The use of SPKFs have also gained acceptance for INS/GPS systems [Ref. 4, 15, 24, 29]. The SPKF again approximates the distribution by a GRV. However, the probability distribution is represented by a set of carefully chosen deterministic sample points. To illustrate the core principle, consider a GRV $x \in R^L$ with mean $\overline{x}$ and covariance $\mathbf{P}$. The sigma point selection scheme can be shown as:
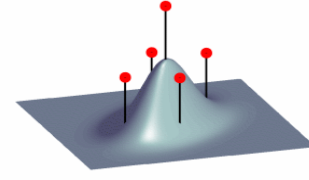

Fig. 3. Weighted sigma points lie along the major eigen-axes of the RV's covariance matrix

$$\chi_0 = \overline{x} \qquad (24)$$

$$\chi_i = \overline{x} + \eta\left(\sqrt{P_x}\right)_i, i = 1\ldots L \qquad (25)$$

$$\chi_i = \overline{x} - \eta\left(\sqrt{P_x}\right)_i, i = L+1\ldots 2L \qquad (26)$$

where η is a scale factor, $\left(\sqrt{P_x}\right)_i$ is the i-th column of the orthogonal covariance matrix square root of P_x, and χ_i is the 2L+1 sigma point set. The sigma point selection scheme for a simple 2-dimensional GRV is shown in Fig. 3. The height of each sigma point indicates its relative weight. These sigma points are then propagated through the true nonlinear system, with the posterior mean and covariance calculated using simple weighted averaging. This deceptively simple approach captures the posterior mean and covariance accurately to the 2nd order (3rd order is achieved for symmetric distribution) for all nonlinearities. In contrast, a linearization based approach (as used in the EKF) achieves only 1st order accuracy. The basic sigma-point propagation scheme is used to form a recursive estimation approach leading to the SPKF. Selection of specific weights for each sigma point and the scale factor η depend on the specific type of SPKF. The computational cost of the SPKF remains the same order as that of EKF. In addition, no analytical Jacobians need be computed, which often makes the SPKF easier to implement than the EKF. For complete equations and a more detailed description, see Ref. 13.

3. THE STATE-DEPENDENT RICCATI EQUATION (SDRE) CONTROLLER

The SDRE approach [Ref. 3] is based on extended linearization of the vehicle dynamics that involves manipulating the dynamic equations

$$\dot{x} = f(x, u) \qquad (27)$$

into a control-affine state-dependent coefficient (SDC) form with state vector x and control u, in which system matrices are explicit functions of the current state

$$\dot{x} = A(x)x + B(x)u \qquad (28)$$

As a trivial example, consider $\dot{x} = \sin x + \cos x\, u$, then $A(x) = \sin x / x$, $B(x) = \cos x$. SDC parameterization

is not unique. Consider $f(x) = A(x)x$, in which case $f(x) = (A(x) + E(x))x$ for any matrix that satisfies $E(x)x = 0$.

The non-uniqueness can affect controllability of the parameterized pair $(A(x), B(x))$. Note however, that controllability of the original dynamics is not guaranteed by this condition alone [Ref. 9]. If the pair $(A(x), B(x))$ is point-wise controllable, then linear system methods can be applied to design a state feedback control, *e.g.* $u = -K(x)x$, that provides $A_c(x) \equiv (A(x) - B(x)K(x)) < 0$. Generally, only local asymptotic stability of the original system is guaranteed without additional conditions. Results from linear time-varying systems theory can be applied to determine stability properties [Ref. 26].

The SDRE design employs an online solution of the standard Riccati Equation to compute the optimal feedback gain matrix $K(x)$, corresponding to the local solution of the linear quadratic (LQ) optimal control problem. The SDRE thus approximates a solution to the LQ optimal control problem

$$u = \text{argmin}\left\{ \int_t^\infty \left(x^T Q x + u^T R u \right) d\tau \right\} \qquad (29)$$

subject to (27)-(28) by solving the linear quadratic regulator (LQR) problem at each t for the linear time-invariant system $A = A(x(t))$ and $B = B(x(t))$, which yields an exact solution to the problem assuming fixed $A(x)$ and $B(x)$ for time $[t, \infty)$.

The SDRE control generally exhibits greater stability and better performance than linear control laws (e.g., LQR), and empirical experience often shows that in many cases the domain of attraction is as large as the domain of interest [Ref. 1, 3].

For digital implementation purposes, we discretize $A(x), B(x)$ into $\Phi(x_k)$, $\Gamma(x_k)$ at every sampling interval and then compute the digital tracking control

$$u_k = -R^{-1} \Gamma^T (x_k) P(x_k) \left(x_k - x_k^{des} \right) + u^{ref}$$
$$\equiv -K(x_k) e_k \qquad (30)$$

where x_k^{des} is a desired state, u^{ref} is a reference input (trim control), and $P(x_k)$ is the solution of the discrete-time algebraic Riccati equation (DARE)

$$\Phi^T \left[P - P\Gamma \left(R + \Gamma^T P \Gamma \right)^{-1} \Gamma^T P \right] \Phi - P + Q = 0 \qquad (31)$$

using state-dependent matrices $\Phi(x_k)$ and $\Gamma(x_k)$, which are treated as being constant at each time step.

For a more detailed treatment of SDRE controllers and the explicit formulation for the helicopter dynamics, the reader is referred to Ref. 2.

4. EXPERIMENTAL RESULTS

While we have recordings from a fully instrumented X-Cell helicopter, all experiments for this initial work were carried out in simulation. This provides more flexibility for evaluations as well as the ability to implement the closed-loop feedback control given the vision-based state estimation. The simulator combines a highly accurate computational flight dynamics model of the helicopter and an OpenGL-based visualization system. The performance is evaluated by comparing the differences between the true state (available from the simulator), the desired state from the controller, and the estimated state. Performance is also compared relative to a simulated on-onboard INS/GPS navigation filter with the same SDRE controller. Simulated maneuvers include rapid turns, climbs, descents and landings.

Fig 4 illustrates the 3D trajectory of the simulated flight for the first closed loop experiment. The desired trajectory of the helicopter consists of several segments: a 360 degree spin at the angular speed 45deg/s, followed by 8 seconds forward at the speed 1m/s, then a vertical climb together with a 180 degree spin, follow by 6 seconds forward at the speed 1m/s, and finally a landing.
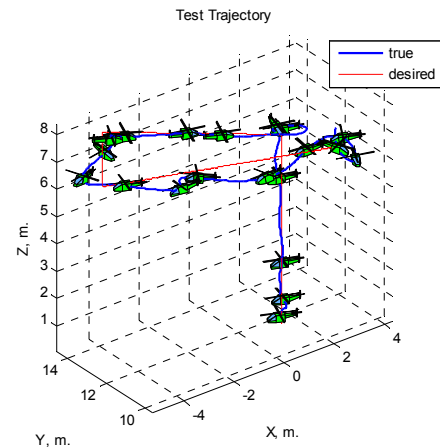

Fig 4. 3D trajectory of the simulated flight for Experiment-1. Vision-only navigation system.
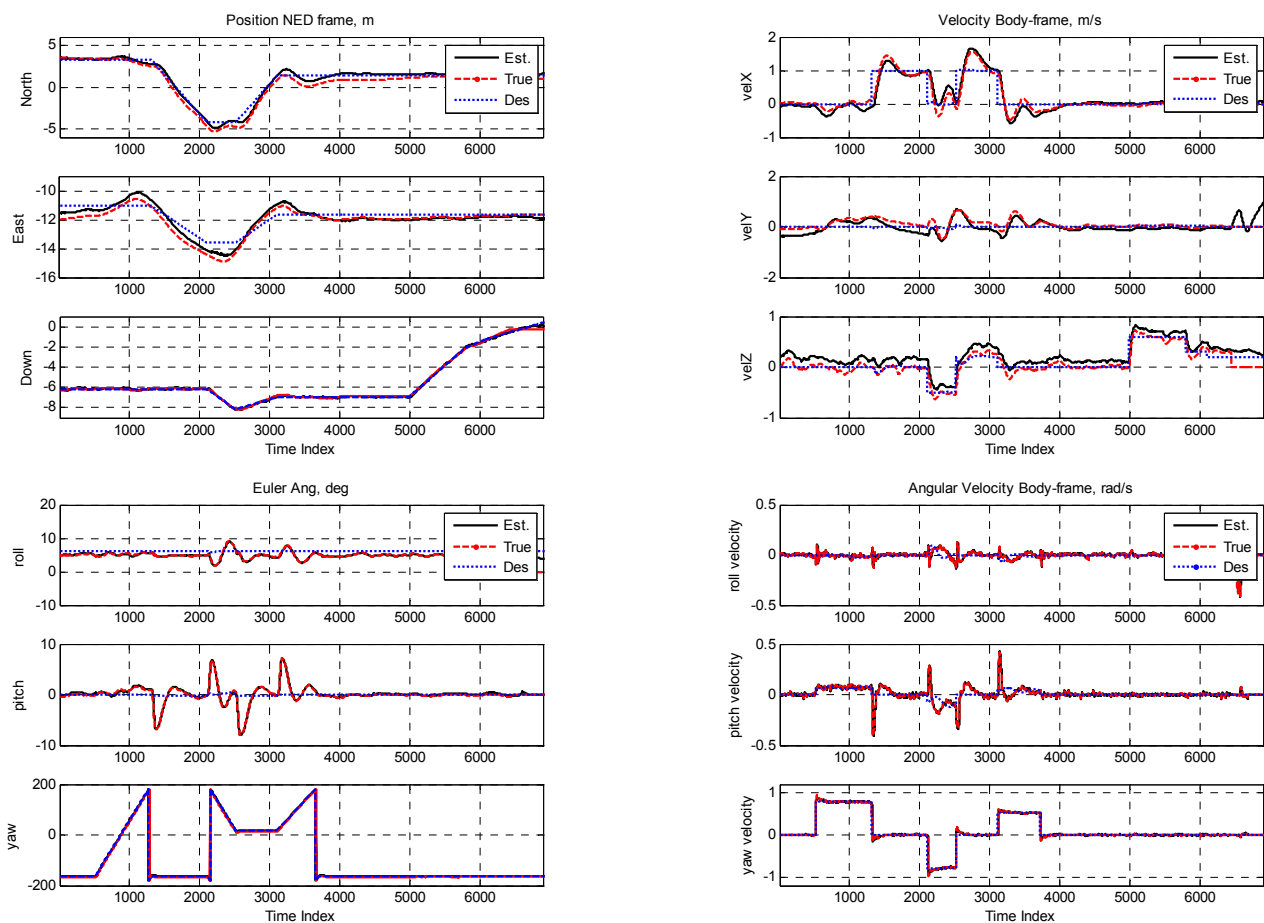
Fig 5a. Experiment-1. INS/GPS integrated navigation system.

Figs 5a and 5b illustrate the comparison between the vision-only navigation system and an INS/GPS integrated navigation system. The full dynamic process model is used for the vision-only navigation system. For the INS/GPS integrated navigation, the update rate of the inertial measurement unit (IMU) is simulated to be 100Hz, the GPS measurements are simulated to update at 10Hz with 50ms delay. In addition, a barometric altimeter is simulated to update at the rate of 5Hz. On the other hand, for the vision-only navigation, the only measurement is the vision measurement extracted from simulated images updated at the rate of 10Hz. The same SDRE controller updated at the rate 50Hz has been used in both cases.

As can be seen from Fig 5, the performance of the vision-only navigation system and the INS/GPS navigation system are quite comparable. The vision-only navigation has smaller estimation error for position and velocity. However, for Euler angles and angular velocities, the performance of the vision-only navigation is slightly worse. This is not surprising, as the IMU provides direct measurements of the angular velocities. For the vision-only navigation and control, the roll angular velocity is especially difficult stabilize. This is due to the geometrical symmetry of the helicopter with respect to the x-axis of the body frame.
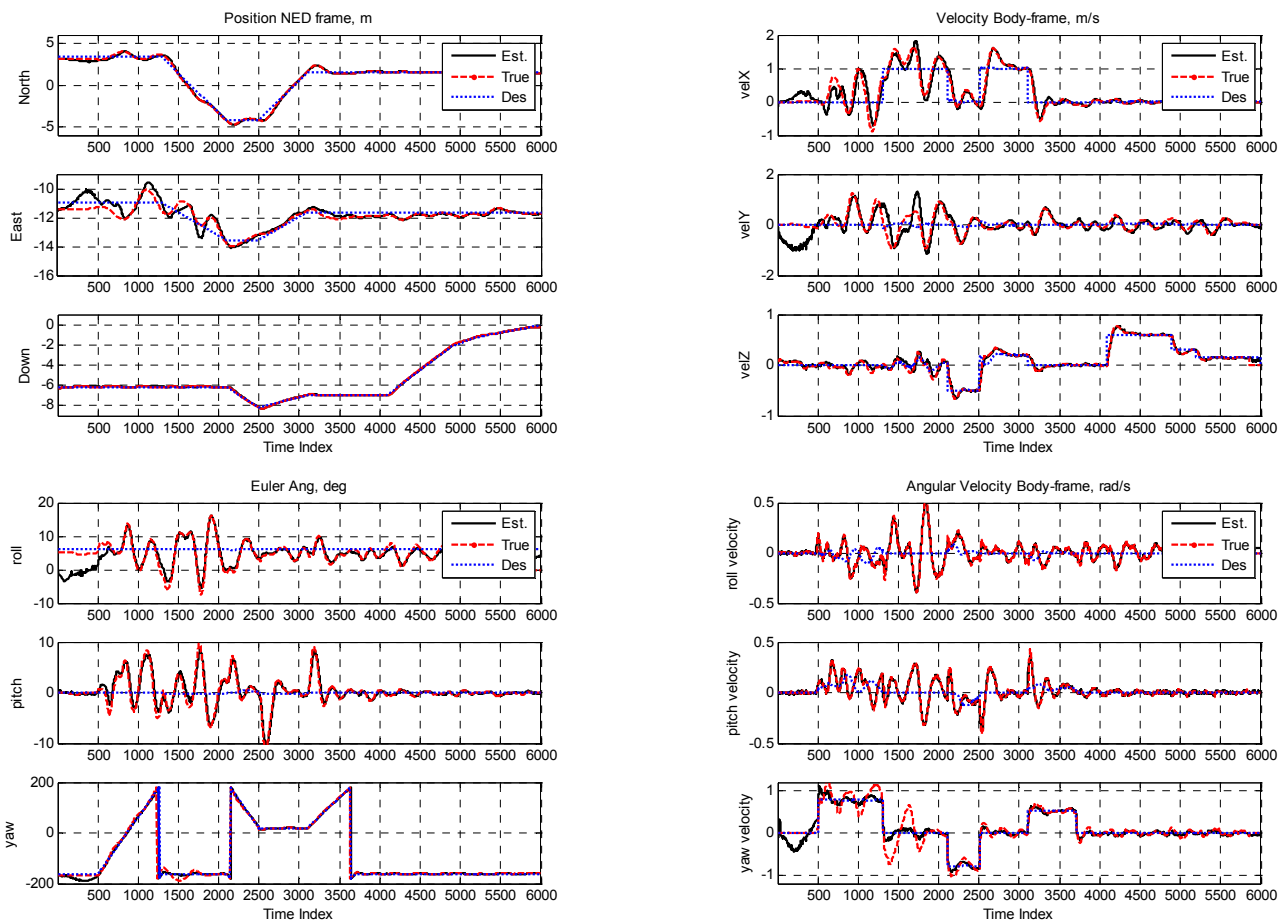
Fig 5bExperiment-1. Vision-only navigation system.

Fig 6 illustrates the 3D trajectory of the simulated flight for the second closed loop experiment. The desired trajectory of the helicopter is nose-in pirouette with a 2 meter radius at 36 deg/second. The comparison of the state variable between the vision-only navigation system and the INS/GPS integrated navigation system is illustrated in Fig 7a and 7b.
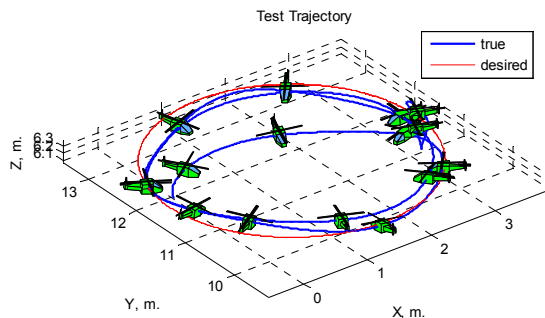

Fig 6. 3D trajectory of the simulated flight for Experiment-2. Vision-only navigation system

Again it is observed that the vision-only navigation system performs similar to the full INS/GPS integrated navigation system. The estimation error for position and velocity of vision-only navigation is smaller. However, the stabilization of roll angle is harder for the vision-only navigation than the INS/GPS integrated navigation, as had been observed earlier.

For both experiments, the dynamic model was used for the SPKF based state estimation. Use of the stochastic process model resulted in an unstable system as illustrated in Fig 8. The divergence of the stochastic model in closed loop may be due to the multi-rate estimator/controller feedback loop in which the vision system operates at 10Hz and the control operates at 50Hz. The model predictions of the stochastic approximation between vision updates are not accurate enough to maintain stability of the helicopter. Note that divergence using the stochastic model was not observed in open-loop (i.e., monitoring the vision-only state-estimation performance without use for feedback control). However, high frequency noise was more apparent in the angular velocity estimates using the stochastic model relative to the dynamic model.
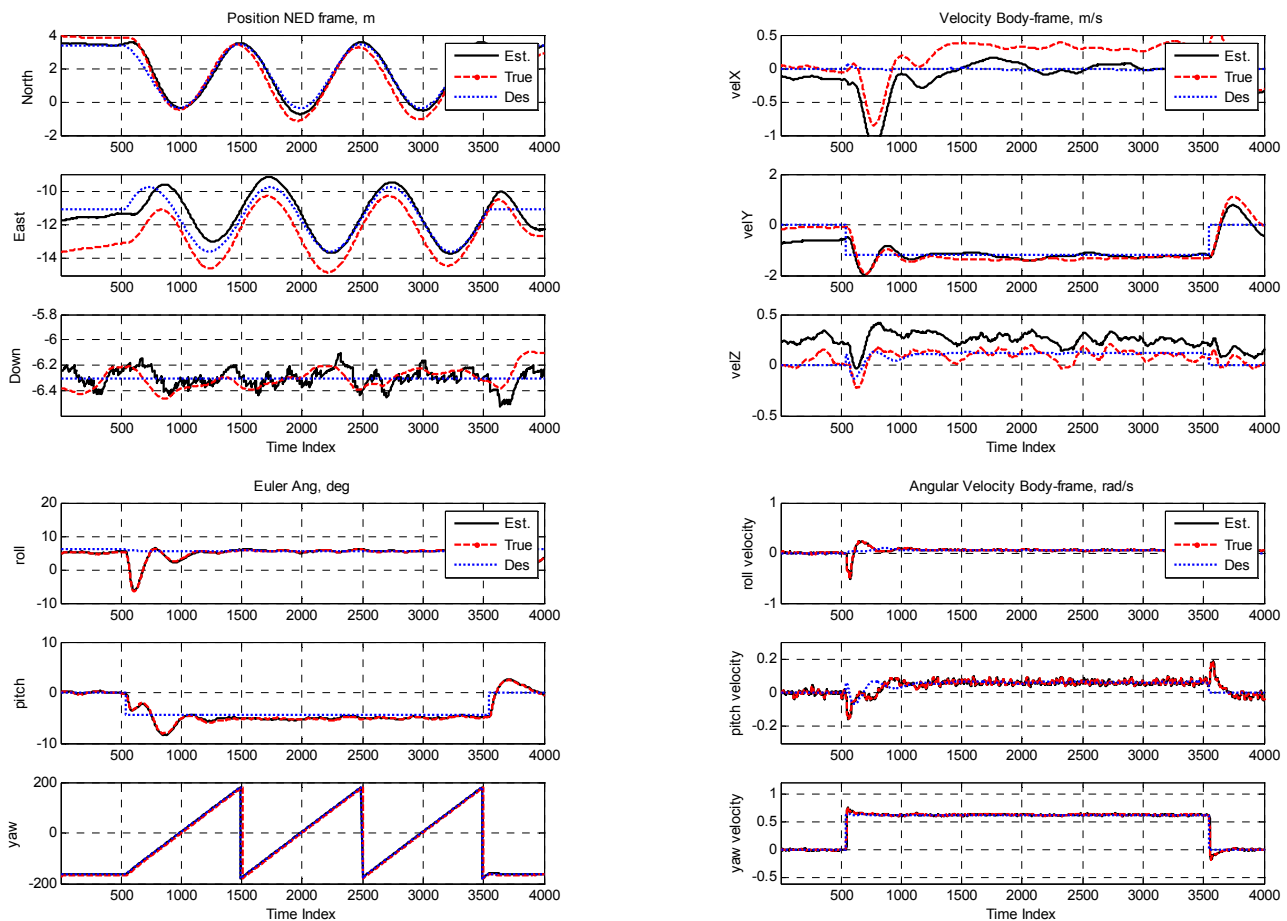
Fig 7a. Experiment-2. INS/GPS integrated navigation system.

The performance of the vision-only navigation system was also tested using an EKF instead of the SPKF. However, the EKF encountered numerical difficulties and often diverged due to larger state-estimation errors.

5. CONCLUSIONS AND FUTURE WORK

The vision-only navigation and control system may provide an alternative to the traditional INS/GPS integrated navigation system for small UAVs. Other than simple on-board avionics for low level actuator control, the ground station is responsible for video capture, state-estimation, and state-feedback flight control.

Our experiments demonstrated the feasibility of designing a vision-only estimation and control system capable of stabilizing and maneuvering a small unmanned helicopter. The estimator/controller feedback loop given only vision measurements from a fixed camera on the ground can successfully stabilize the helicopter as it executes a series of maneuvers including rapid turns, climbs, descents and landings.

Key to the successful closed-loop performance was the use of an accurate dynamic process model for the vehicle's state estimation. In addition, it was necessary to use the more accurate SPKF instead of the common EKF. Algorithmic extensions currently under investigation include the use of active contours for image features as well as applying sigma-point particle filters for state estimation.
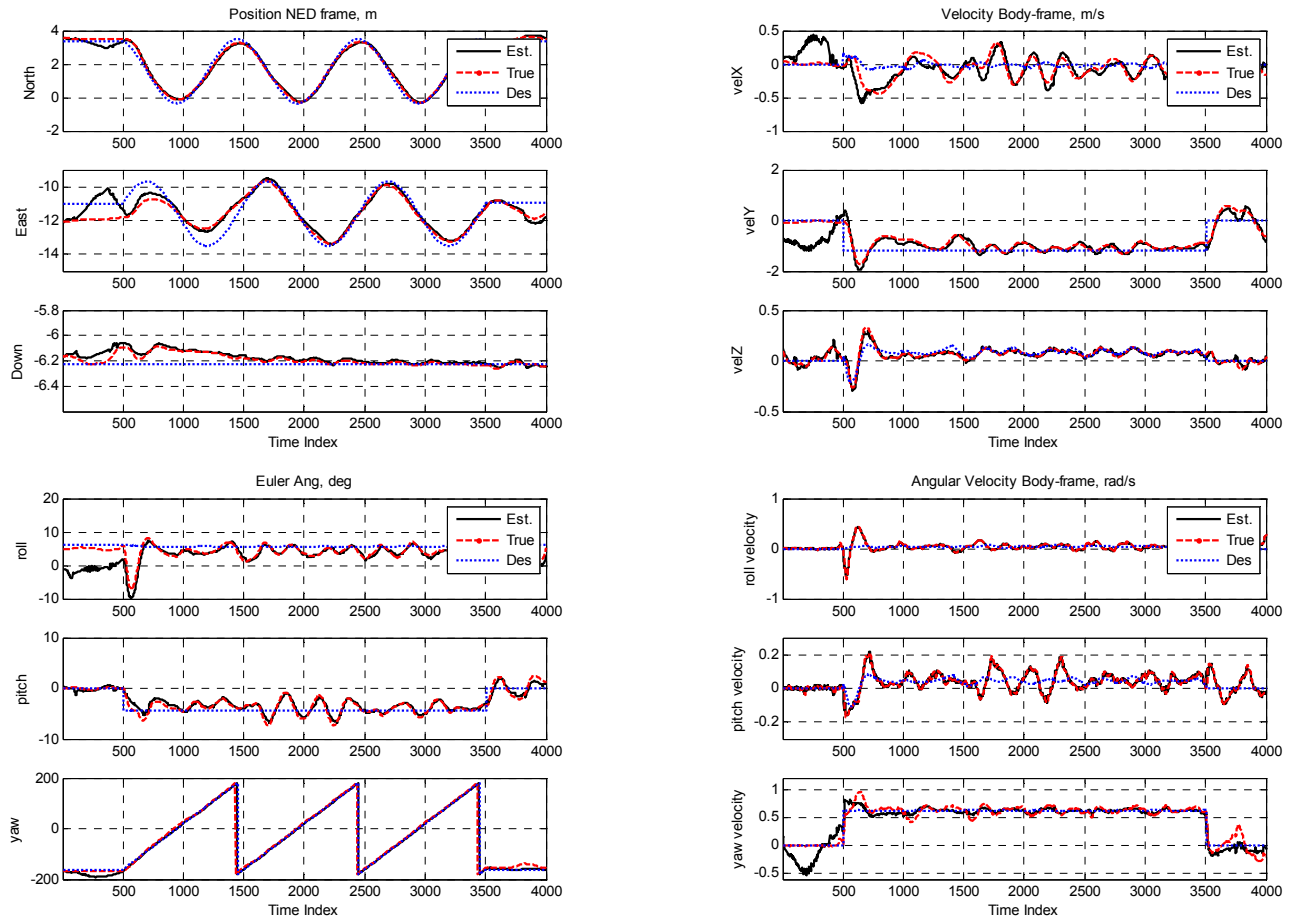
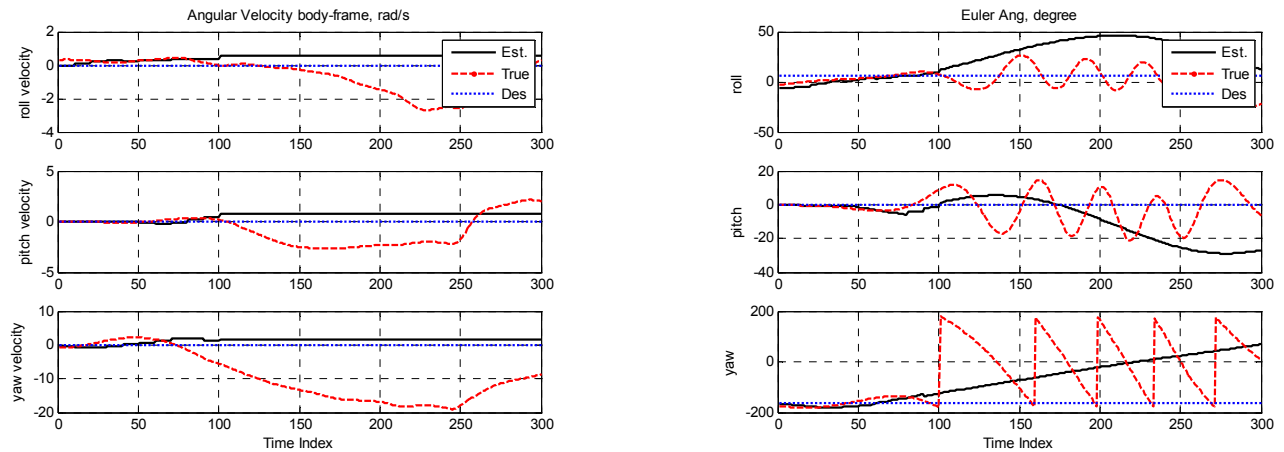**Fig 7b. Experiment-2. Vision-only navigation system.**

Fig 8. Divergence of the stochastic model with closed loop control.

ACKNOWLEDGMENTS

REFERENCES

1 A. Bogdanov, Optimal control of a double inverted pendulum on a cart. Tech. Rep. CSE-04-006, OGI School of Science & Engineering, OHSU, December 2004.

2 A. Bogdanov, E. Wan, State-dependent Riccati equation control for small autonomous helicopters. Journal of Guidance, Control, and Dynamics, 2007 vol. 30 no. 1

3 J. R. Cloutier, C. N. D'Souza, and C. P. Mracek, Nonlinear regulation and nonlinear H-infinity control via the state-dependent Riccati equation technique: Part1, Theory. Proceedings of the International Conference on Nonlinear Problems in Aviation and Aerospace, Daytona Beach, FL, May 1996.

4 J. L. Crassidis, Sigma-Point Kalman Filtering for Integrated GPS and Inertial Navigation, AIAA Guidance, Navigation, and Control Conference, San Francisco, CA, August, 2005.

5 E. W. Frew. Observer Trajectory Generation for Target-Motion Estimation Using Monocular Vision. PhD thesis, Stanford University, Stanford, CA, August 2003

6 E. W. Frew, J. Langelaan, S. Joo. Adaptive Receding Horizon Control for Vision-Based Navigation of Small Unmanned Aircraft. 2006 American Control Conference, Minneapolis, June 2006.

7 V. Gavrilets, B. Mettler, E. Feron. Dynamic Model for a Miniature Aerobatic Helicopter. AIAA Guidance Navigation and Control Conference, Montreal, Canada, August 2001.

8 M. Grewal, L. R. Weil, and A. P. Andrews, Global Positioning Systems, Inertial Navigation and Integration, 1st ed: John Wiley & Sons, 2001.

9 K. D. Hammett, C. D. Hall, and D. B. Ridgely, Controllability Issues in Nonlinear State-Dependent Riccati Equation Control. Journal of Guidance, Control and Dynamics. Vol. 5, No. 21, September-October 1998, pp. 767-773.

10 S. J. Julier and J. K. Uhlmann, Unscented Filtering and Nonlinear Estimation, In Proceedings of the IEEE, vol. 92, pp. 401-422, March 2004.

11 J. J. Kehoe, R. S. Causey, M. Abdulrahim, R. Lind. Waypoint Navigation of a Micro Air Vehicle using Vision-Based Attitude Estimation. AIAA Guidance, Navigation and Control Conference, San Francisco, CA, August 2005

12 X. R. Li, V. P. Jilkov. Survey of Maneuvering Target Tracking Part I: Dynamic Models. IEEE Trans. on Aerospace and Electronic Systems, vol.39, No.4, Oct. 2003

13 R. van der Merwe. Sigma-Point Kalman Filters for Probabilistic Inference in Dynamic State-Space Models. Ph.D Thesis, OGI School of Science & Engineering, Oregon Health & Science University, April 2004.

14 R. van der Merwe and E. Wan, The Square-Root Unscented Kalman Filter for State and Parameter Estimation, In Proceedings of the IEEE International Conference on Acoustics, Speech and Signal Processing (ICASSP), vol. 6, pp. 3461-3464, Salt Lake City, UT, May 2001.

15 R. van der Merwe, E. Wan, S. Julier, A. Bogdanov, G. Harvey, and J. Hunt, Sigma-Point Kalman Filters for Nonlinear Estimation and Sensor Fusion: Applications to Integrated Navigation, in Proceedings of the AIAA Guidance Navigation & Control Conference, August 2004.

16 R. Mohr, B. Triggs. Projective Geometry for Image Analysis - A Tutorial given at ISPRS, Vienna, July 1996. http://homepages.inf.ed.ac.uk/rbf/CVonline/LOCAL_CO PIES/MOHR_TRIGGS/isprs96.html

17 L. Muratet, S. Doncieux, Y. Brière, and J.-A. Meyer. A contribution to vision-based autonomous helicopter flight in urban environments. *Robotics and Autonomous Systems*, 50(4):195-209. 2005

18 M. Norgaard, N. Poulsen, and O. Ravn, "New Developments in State Estimation for Nonlinear Systems," Automatica, vol. 36, pp. 1627-1638, November 2000.

19 R. J. Prazenica, A. Watkins, A. J. Kurdila, Q. F. Ke, T. Kanade. Vision-Based Kalman Filtering for Aircraft State Estimation and Structure from Motion. AIAA Guidance, Navigation, and Control Conference and Exhibit, August 2005, San Francisco, California

20 A. A. Proctor, E. N. Johnson. Vision-only Approach and Landing. AIAA Guidance, Navigation, and Control Conference and Exhibit, August 2005, San Francisco, California

21 A. A. Proctor, E. N. Johnson. Vision-only Aircraft Flight Control Methods and Test Results. AIAA

Guidance, Navigation, and Control Conference and Exhibit, August 2005, San Francisco

22 S. Saripalli, J. F. Montgomery, G. S. Sukhatme. Visually-Guided Landing of an Unmanned Aerial Vehicle. IEEE Transactions on Robotics and Automation, Vol. 19, No. 3, pp. 371-381, Jun 2003

23 G. Scott and H. Longuet-Higgins. An algorithm for associating the features of two patterns. Proc. Royal Society London, volume B244, 1991.

24 E.-H. Shin, X. Niu, and N. El-Sheimy, Performance Comparison of the Extended and the Unscented Kalman Filter for Integrated GPS and MEMS-Based Inertial Systems, ION National Technical Meeting, San Diego, CA, January, 2005

25 B. Sinopoli, M. Micheli, G. Donato, T. J. Koo. Vision Based Navigation for an Unmanned Aerial Vehicle. Proc. of the IEEE International Conference on Robotics and Autoation (ICRA 2001), Seoul, Korea, May 2001

26 J.-J. E. Slotine, W. Li, Applied nonlinear control. Prentice-Hall, Englewood Cliffs, NJ, 1991.

27 D. H. Titterton, J. L. Weston. Strapdown Inertial Navigation Technology. Peter Peregrinus Ltd. 1997

28 C. D. Wagter, J. A. Mulder. Towards Vision-Based UAV Situation Awareness. AIAA Guidance, Navigation, and Control Conference, 15-18 Aug 2005, San Francisco

29 Y. Yi, D. A. Grejner-Brzezinska, Tightly-coupled GPS/INS Integration Using Unscented Kalman Filter and Particle Filter, ION GNSS 2006